

Electrowetting devices with transparent single-walled carbon nanotube electrodes

Liangbing Hu and George Gruner^{a)}

Department of Physics and Astronomy, University of California Los Angeles, Los Angeles, California, 90095

Jian Gong and Chang-Jin "CJ" Kim

Department of Mechanical and Aerospace Engineering, University of California Los Angeles, Los Angeles, California 90095

Bjoern Hornbostel

Max-Planck-Institute for Solid State Research Heisenbergstrasse 1, Stuttgart 70569, Germany

(Received 1 December 2006; accepted 18 January 2007; published online 2 March 2007)

Microfluidic devices based on the electrowetting principle, more specifically electrowetting on dielectric, were fabricated using transparent single-walled carbon nanotube films as electrodes. The films were spray coated on glass and polyethylene terephthalate substrates. The transmittance and sheet resistance remain unchanged after patterning the films using typical photolithography and plasma etching. Operation of water droplets over the patterned nanotube electrodes was demonstrated, and the performance was found to be comparable to that over the usual metal electrodes. The requirement of transparent electrodes is estimated for displays based on electrowetting mechanism, and nanotube films indicate promise for such a type of devices. © 2007 American Institute of Physics. [DOI: 10.1063/1.2561032]

Electrowetting is a promising principle for the generation of microscale fluid movement, currently led by the configuration of electrowetting on dielectric (EWOD).¹ Wettability of a solid surface increases when a voltage is applied between the surface and a conducting liquid on it. Under certain circumstances, a motion of droplets can be induced. The technology has been used for many applications including electronic papers,² adaptive lenses,³ and optical filters.⁴ Most electrowetting applications today use the configuration of EWOD: a patterned conducting layer covered with a dielectric layer and coated with a highly hydrophobic layer on top. For the optical applications such as displays and some lab-on-chip (LOC) applications, the device needs to be transparent to be seen or observed, requiring transparent and electrically conducting substrates. Indium tin oxide (ITO) is commonly used for the electrodes when fabricating transparent electrowetting devices.

Transparent and conducting films made of randomly distributed single-walled carbon nanotubes (SWCNTs) have shown promise as a candidate to replace ITO.⁵ Devices such as organic light emitting diodes,⁶ solar cells,⁷ and transistors⁸ having transparent nanotube layers have been demonstrated. Typically, the sheet resistance (R_s) of a SWCNT film is in the range of 100–1000 Ω /sq with 80% transmittance in the visible range, while R_s of ITO is less than 100 Ω /sq on glass and 100–300 Ω /sq on polyethylene terephthalate (PET). The major concern with replacing ITO with nanotube films in electrowetting devices is their higher sheet resistance than ITO at the same transparency. The effect of the high sheet resistance on the speed of an electrowetting device and the voltage drop in the electrode are analyzed. Figure 1(a) shows the configuration of the EWOD device we fabricated, where

the conducting materials are SWCNT films. The equivalent circuit is shown in Fig. 1(b). A high voltage—direct current (dc) or alternative current (ac)—is applied to the EWOD electrodes to charge the dielectric layer (with capacitance C_d) through the nanotube electrode lines with connecting resistance R_c . A liquid droplet with resistance R_w and capacitance C_w is sandwiched between the EWOD electrode and ground electrode. Here we ignore the capacitance of Teflon layer due to the fact that the spin-coated Teflon has many pin holes. The liquid resistance and capacitance depend on the type of solution and ion concentration. For typical ionic water solution (e.g., 0.01–1M KCl), C_w can be ignored and R_w is in the 1–500 Ω range.⁹ C_d is in the 1 pF–1 nF range in microflu-

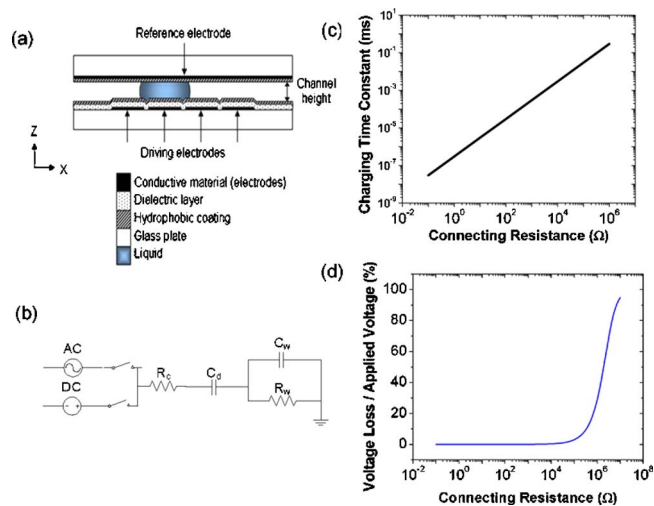


FIG. 1. (Color online) (a) Cross-sectional schematic of an EWOD device (adapted from Ref. 2). (b) Equivalent circuit for the EWOD configuration (adapted from Ref. 1). (c) dc charging time constant for EWOD activation vs connecting resistance. (d) ac voltage loss during EWOD activation vs connecting resistance.

^{a)} Author to whom correspondence should be addressed; electronic mail: ggruner@ucla.edu

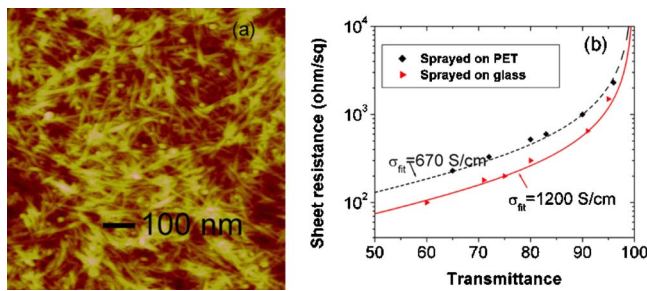


FIG. 2. (Color online) (a) AFM image of sprayed nanotube film with $R_s = 500 \Omega/\text{sq}$. (b) Sheet resistance vs transmittance for sprayed nanotube films on two transparent substrates (glass wafer and PET). The data are fitted to Eq. (1).

idics devices when the electrode is small ($<10 \text{ mm}$) and the dielectric layer is thin ($<1 \mu\text{m}$).¹⁰ In our devices, the electrode is $1.5 \times 1.5 \text{ mm}^2$ in dimension, the dielectric is 500 nm thick Si_3N_4 , and the hydrophobic layer is 200 nm thick AF1600 Teflon. The calculated C_d per electrode pad is approximately 30 pF . For an applied dc signal [Fig. 1(c)], the capacitor charging time constant $R_c C_d$ is less than 1 ms even for a $1 \text{ M}\Omega$ resistance, which is fast enough for typical display applications (refresh rate is usually less than 100 Hz). For an applied ac signal, high connecting resistance could lead to high voltage drop, which in turn reduces the voltage applied to the electrode and subsequently deteriorates the EWOD performance. At the typical driving frequency (1 kHz) in Fig. 1(d), a connecting resistance less than $10 \text{ k}\Omega$ would have minor effect (less than 1%), and $1 \text{ M}\Omega$ would yield an approximate 30% voltage drop.

SWCNT films were spray coated on the glass and PET substrates. Arc-discharged nanotube powders purchased from Carbon Solution Inc. were dispersed in water with 1% weight sodium dodecyl sulphate and sprayed onto the substrates that have been heated to 80°C . Before the spraying, the substrates need to be soaked in 1% weight 3-aminopropyltriethoxysilane (silane) water solution for 5 min to improve the adhesion of nanotube films to the substrates. Figure 2(a) shows the atomic force microscope (AFM) image of films on glass substrate. The transmittance of sprayed nanotube films can be tuned simply through the spraying steps and the solution concentrations. Typically, five spraying steps with 1 mg/mL nanotube solutions will result in films with 80% transmittance. The sheet resistance and transmittance at 550 nm wavelength are plotted and fitted by Eq. (1) [Fig. 2(b)], leading to dc conductivity of 670 S/cm for films on PET and 1200 S/cm on glass, higher than the reported data.¹¹ Higher conductivity achieved on the glass substrate may be due to its smoother surface than the PET substrate.

$$T = \left(1 + \frac{188 (\Omega) 200 (\text{S/cm})}{R_s \sigma_{\text{dc}}} \right)^{-2}. \quad (1)$$

Photolithography and O_2 plasma have been employed to pattern transferred nanotube films from a filter membrane.¹² The patterned film's size is limited to that of the membrane. However, the sprayed film coverage area can be as large as the substrate. We tested various types of plasma and found that Ar , O_2 , CF_4 , or CF_6 plasma can effectively etch nanotubes. The fabrication steps are shown in Fig. 3(a). First, the nanotube films are spray coated, and then photoresist (PR) is spin coated on top, exposed, and developed. After photoli-

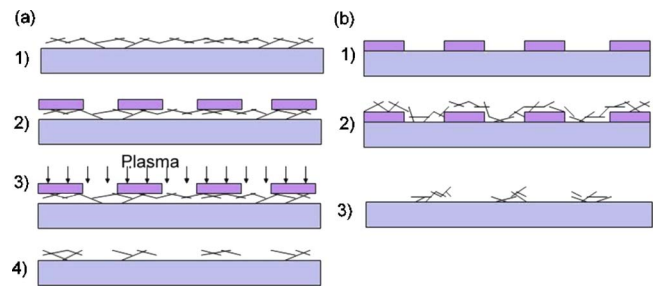


FIG. 3. (Color online) (a) Process sequence used for patterning nanotube films. (1) Treat transparent substrate with silane and spray nanotubes on it, (2) pattern PR, (3) plasma etch nanotubes, and (4) remove PR with acetone. (b) An alternative process (lift-off) for obtaining patterned nanotube films. (1) Pattern PR, (2) treat the substrate with silane and spray nanotube films, and (3) remove PR.

thography, gas plasma within a reactive ion etcher (RIE) system (i.e., 100 W rf power and 5 min etching with Ar plasma) removes the nanotubes in the unprotected areas. Finally the PR is stripped off by acetone, and the sample is rinsed in de-ionized (DI) water and blown with nitrogen gas to dry. An alternative method to fabricate patterned films is the lift-off process [Fig. 3(b)]. In this method, PR is first patterned, and the substrate is then treated with silane solution. The nanotube film is sprayed over the substrate and the remaining PR is removed by soaking the substrate in acetone. Finally, the substrate is rinsed in DI water and blown to dry.

We applied both methods to deposit patterned nanotube films. Figure 4(a) shows a patterned nanotube film on a 4 in. glass wafer and (b) shows a patterned film on a PET flexible substrate. The square pads visible in the pictures are gold contact pads; the nanotube thin-film electrodes are vaguely visible. Patterning resolution of $4 \mu\text{m}$ is achieved on both substrates [shown in Fig. 4(c)]. There are no distinguishable changes in sheet resistance and transmittance observed before and after repeating the lithographic patterning process five times. Figure 4(d) displays the transmittance of films before and after the patterning using method (a), where the

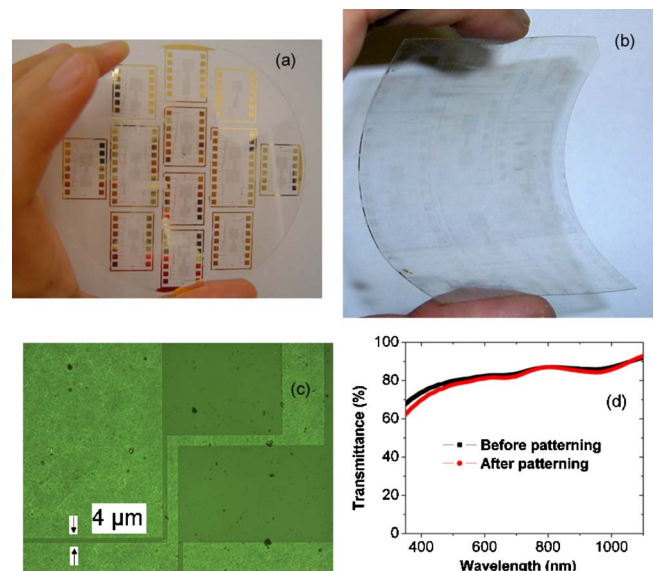


FIG. 4. (Color online) (a) Patterned nanotube films on 4 in. glass wafer. (b) Patterned films on flexible PET substrate. No gold patterns here. (c) Enlarged image of the patterned nanotube lines. (d) Transmittance vs wavelength for nanotube films before and after lithographic patterning. Note that the sheet resistance changes little after patterning the films.

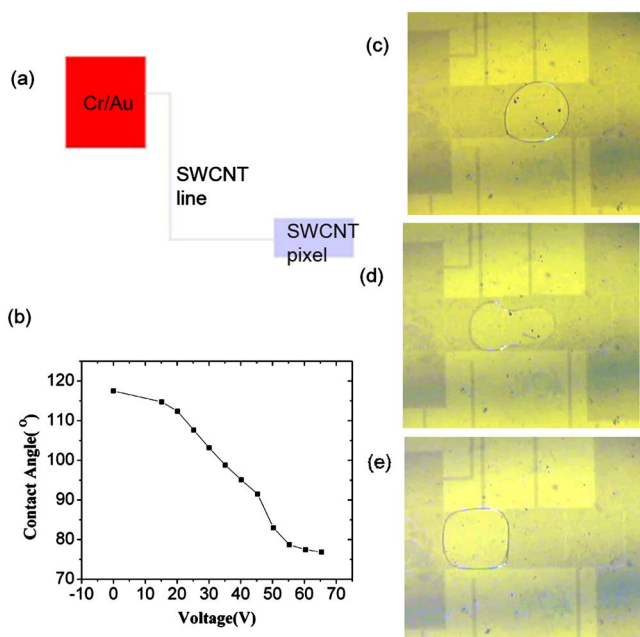


FIG. 5. (Color online) (a) Schematic drawing for a gold contact pad and a nanotube pixel, connected through a $100\ \mu\text{m}$ wide nanotube line. (b) Contact angle vs applied voltage through nanotube pixel area. [(c)–(e)] Sequential images showing droplet movement. The droplet size is approximately 1 mm.

sheet resistance of the films is $300 \pm 30\ \Omega/\text{sq}$. It is important to treat the substrate before spraying nanotubes to achieve good adhesion; the nanotubes were found to peel off from untreated substrates after the patterning process. The compatibility of spraying nanotube films with photolithography and various plasma etching recipes offers a simple method to fabricate patterned nanotube films with high resolution.

To test nanotube films as the transparent conducting layers for electrowetting applications, we made EWOD devices using the configuration shown in Fig. 1(a). The steps are given as follows. (1) Spray coat nanotube films (80% transmittance) on 4 in. glass or PET substrates; (2) evaporate and lithographically pattern (by wet etching) the 20 nm Cr/200 nm Au as electrical contact pads for applying driving voltage; (3) lithographically pattern (by plasma RIE) the nanotube film to define EWOD pixel electrodes; (4) coat 500 nm Si_3N_4 as dielectric layer by plasma-enhanced chemical-vapor deposition, and open the contact pads by CF_4/O_2 RIE pattern; (5) spin coat 200 nm AF1600 Teflon as the top hydrophobic layer. AFM image of the Teflon coated on a nanotube film reveals a 5 nm roughness, comparable with the roughness (2.5 nm) of Teflon spin coated on an ITO/glass substrate; and (6) dice 4 in. glass or PET substrate into pieces for electrowetting tests. Figure 4(a) shows the 4 in. glass wafer with 12 devices before the dicing.

We evaluated the contact resistance between the metal pad and the patterned nanotube lines, because it can also be a source of high resistance between the applied voltage and EWOD electrodes. By probing the metal pad and nanotube pixel area [Fig. 5(a)], the measured resistance was 20 k Ω , which includes R_{metal} , R_{contact} , and R_{nanotube} . The dimension of the Au pad is $2 \times 2\ \text{mm}^2$ with 200 nm thickness, and the nanotube line is $100\ \mu\text{m}$ wide, 7 mm long, and 30 nm thick. Au conductivity is $0.45 \times 10^6\ \text{S/cm}$, and sprayed nanotube conductivity on glass is 1200 S/cm. Thus the Au pad resistance is only several ohms, and the nanotube line resistance

is 19.4 k Ω . The contact resistance of a $100\ \mu\text{m}$ wide nanotube film with Au pad is about 0.6 k Ω , which is more than 20 times less than the resistance of the nanotube line.

To verify the electrowetting principle, we first measured contact angle versus applied voltage for pure water on SWCNT devices. Contact angles were measured by an optical contact angle measurement system (FTA 1000) and the measured data [Fig. 5(b)] follow the same trend found with metal electrodes.¹ We also tested the droplet translation on the nanotube EWOD devices. To provide the electrical ground, 200 nm AF1600 Teflon was spin coated onto a non-patterned nanotube glass plate and used as the top plate shown in Fig. 1(a). A 200 nL droplet was then sandwiched between the two parallel plates with a $100\ \mu\text{m}$ spacer. Then, through the corresponding Cr/Au contact pads, a 50 V_{dc} voltage was applied to the desired EWOD electrode to translate the droplet toward it. Figures 5(c)–5(e) show snapshots of a droplet translated between the electrodes. Droplet translation rate was as fast as that of devices using ITO electrodes in a similar condition (10 mm/s).²

In conclusion, we tested patterned nanotube films as electrodes in EWOD devices, the performance of which was indistinguishable from those obtained from ITO electrode devices. We also evaluated the effect of high sheet resistance on the time delay and the voltage drop and found that high sheet resistance up to 10 k Ω/sq has negligible effect. Therefore, highly conductive ITO is not necessary and, under certain circumstances, not suitable. For example, in flexible device applications based on the electrowetting mechanism, such as electronic paper, highly conducting ITO is normally around 100 nm thick and easy to crack. However, thinner ITO is difficult to form into a continuous conducting network due to its one-dimensional properties. For nanotubes with high length/width ratio, the percolation threshold is extremely small and a conducting network is formed at low coverage.⁵ Even such a monolayer, nanotube network will be conductive enough for EWOD-type devices and obviously will possess near-perfect optical transparency.

This work has been supported by NSF Grant No. DMR-040429 and the NASA Institute for Cell Mimetic Space Exploration (CMISE) at UCLA. Two of the authors (L.H. and J.G.) have equally contributed in this work.

¹H. Moon, S. K. Cho, R. L. Garrel, and C.-J. Kim, J. Appl. Phys. **92**, 4080 (2002).

²R. A. Hayes and B. J. Feenstra, Nature (London) **425**, 383 (2003).

³B. Berge and J. Peseux, Eur. Phys. J. E **3**, 159 (2000).

⁴M. W. J. Pins, W. J. J. Welters, and J. W. Weekamp, Science **291**, 277 (2001).

⁵Z. C. Wu, Z. H. Chen, X. Du, J. M. Logan, J. Sippel, M. Nikolou, K. Kamaras, J. R. Reynolds, D. B. Tanner, A. F. Herbard, and A. G. Rinzler, Science **305**, 1273 (2004).

⁶J. Li, L. Hu, L. Wang, Y. Zhou, G. Gruner, and T. J. Marks, Nano Lett. **6**, 2472 (2006).

⁷M. W. Rowell, M. A. Topinka, M. D. McGehee, H. All, G. Dennler, N. S. Saricifceti, L. Hu, and G. Gruer, Appl. Phys. Lett. **88**, 233506 (2006).

⁸Q. Cao, S. H. Hur, Z. T. Zhu, Y. G. Sun, C.-J. Wang, M. A. Meitl M. Shim, and J. A. Rogers, Adv. Mater. (Weinheim, Ger.) **18**, 304 (2006).

⁹K. W. Pratt, W. F. Koch, Y. C. Wu, and P. A. Berezansky, Pure Appl. Chem. **73**, 1783 (2001).

¹⁰S. Cho, H. Moon, and C.-J. Kim, J. Microelectromech. Syst. **12**, 70 (2003).

¹¹E. Bekyarova, M. E. Itkis, N. Cabrera, B. Zhao, A. Yu, J. Gao, and R. C. Haddon, J. Am. Chem. Soc. **127**, 5990 (2005).

¹²S. Lu and B. Panchapakesan, Appl. Phys. Lett. **88**, 253107 (2006).